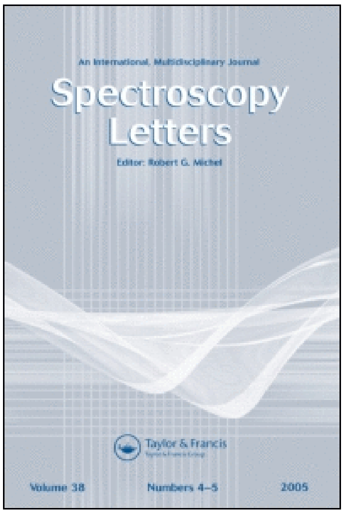

Spectroscopy Letters
Publication details, including instructions for authors and subscription information:
http://www.informaworld.com/smpp/title~content=t713597299

The VUV-VIS Spectroscopic Properties of Dy^{3+} Ion in Phosphors $M_{5-2X}Dy_XNa_X(PO_4)_3F$ (M=Ca, Sr, Ba) and Their Potential Applications in Mercury-Free Lamps

Hongbin Liang[a]; Qu Zeng[a]; Qiang Su[a]; Huihong Lin[a]; Zifeng Tian[a]; Guobin Zhang[b]; Yibing Fu[b]
[a] MOE Laboratory of Bioinorganic and Synthetic Chemistry, State Key Laboratory of Optoelectronic Materials and Technologies, School of Chemistry and Chemical Engineering, Sun Yat-sen University, Guangzhou, China [b] National Synchrotron Radiation Laboratory, University of Science and Technology of China, Hefei, China

To cite this Article Liang, Hongbin , Zeng, Qu , Su, Qiang , Lin, Huihong , Tian, Zifeng , Zhang, Guobin and Fu, Yibing(2007) 'The VUV-VIS Spectroscopic Properties of Dy^{3+} Ion in Phosphors $M_{5-2X}Dy_XNa_X(PO_4)_3F$ (M=Ca, Sr, Ba) and Their Potential Applications in Mercury-Free Lamps', Spectroscopy Letters, 40: 2, 317 — 331

To link to this Article: DOI: 10.1080/00387010701247589

URL: http://dx.doi.org/10.1080/00387010701247589

Spectroscopy Letters, 40: 317–331, 2007

ISSN 0038-7010 print/1532-2289 online
DOI: 10.1080/00387010701247589

The VUV-VIS Spectroscopic Properties of Dy^{3+} Ion in Phosphors $M_{5-2X}Dy_XNa_X(PO_4)_3F$ (M = Ca, Sr, Ba) and Their Potential Applications in Mercury-Free Lamps

Hongbin Liang, Qu Zeng, Qiang Su, Huihong Lin, and Zifeng Tian
MOE Laboratory of Bioinorganic and Synthetic Chemistry, State Key Laboratory of Optoelectronic Materials and Technologies, School of Chemistry and Chemical Engineering, Sun Yat-sen University, Guangzhou, China

Guobin Zhang and Yibing Fu
National Synchrotron Radiation Laboratory, University of Science and Technology of China, Hefei, China

Abstract: The phosphors, fluorapatites $M_5(PO_4)_3F$ (M = Ca, Sr, Ba) activated with Dy^{3+} ions, were prepared by a high-temperature solid-state reaction technique. The VUV-UV excitation spectra and emission spectra under VUV/UV excitation were measured. The phosphors show broad and strong absorption near 172 nm and intensive emission with the chromaticity coordinates entering the white light region. Hence, the phosphors may be considered as suitable candidates for Hg-free lamps.

Keywords: $Ba_5(PO_4)_3F$, $Ca_5(PO_4)_3F$, Dy^{3+}, $Sr_5(PO_4)_3F$, luminescence, vacuum ultraviolet

Received 28 May 2006, Accepted 30 July 2006

The authors were invited to contribute this paper to a special issue of the journal entitled "Spectroscopy of Lanthanide Materials." This special issue was organized by Professor Peter Tanner, City University of Hong Kong, Kowloon.

Address correspondence to Qiang Su, MOE Laboratory of Bioinorganic and Synthetic Chemistry, State Key Laboratory of Optoelectronic Materials and Technologies, School of Chemistry and Chemical Engineering, Sun Yat-sen University, Guangzhou 510275, China. E-mail: suqiang@mail.sysu.edu.cn

INTRODUCTION

Tricolor lamps are widely used in various places. In these lamps, the white-emitting light is commonly obtained by three phosphors, viz. the blend of red-emitting phosphor Y_2O_3:Eu^{3+} (YOE), the green-emitting Zn_2SiO_4:Mn^{2+} (ZSM), $CeMgAl_{11}O_{19}$:Tb^{3+} (CAT), (La,Ce)PO_4:Tb^{3+} (LAP), or (Ce,Gd)Mg B_5O_{10}:Tb^{3+} (CBT), and the blue-emitting $BaMgAl_{10}O_{17}$:Eu^{2+} (BAM).[1,2] The main drawback of these lamps is that the electric discharge of Hg atoms is used as excitation source, and it is harmful to the environment. Hence a new approach, a mercury-free lamp, has been proposed in recent years. The plasma of the mixture of Xe-containing noble gases provides the excitation source in mercury-free lamp. The main emission of this plasma consists of vacuum ultraviolet (VUV; wavelength $\lambda < 200$ nm, energy $E > 50{,}000\,cm^{-1}$) 147 and 172 nm bands. The tricolor phosphors, (Y,Gd)BO_3:Eu^{3+} (YGB) with red emission, Zn_2SiO_4:Mn^{2+} (ZSM) with green emission, and $BaMgAl_{10}O_{17}$:Eu^{2+} (BAM) with blue emission, are usually recommended to be used in these lamps and plasma display panel (PDP) devices.[3,4]

The aim of the current investigation is to develop a novel approach for a mercury-free lamp, in which the white light emission can be realized by a single phosphor, and the phosphor is doped with only one type of activation ions, Dy^{3+}. In order to fulfill this purpose, the fluorapatites $M_5(PO_4)_3F$ (M = Ca, Sr, Ba) were chosen as host compound.

$M_5(PO_4)_3F$ are well-known for their lighting importance. The phosphors $Ca_5(PO_4)_3X$:Sb^{3+},Mn^{2+} (X = F, Cl) were invented in 1942 and have been the main phosphors in fluorescent lamps until now.[1,2] Because of the excellent luminescence of these phosphors, the spectroscopic properties of rare-earth-ions–doped $M_5(PO_4)_3F$ have been extensively studied. However, to our knowledge the luminescent properties of $M_5(PO_4)_3F$:Dy under VUV excitation was not reported.

Dy^{3+} is abundant in the ion adsorption type deposit of China. Its price is cheap. Dy^{3+} ion has two dominant bands in the emission spectrum. The yellow band (575 nm) corresponds with the hypersensitive transition ${}^4F_{9/2} \rightarrow {}^6H_{13/2}$ ($\Delta L = 2$, $\Delta J = 2$), and the blue band (480 nm) corresponds with the ${}^4F_{9/2} \rightarrow {}^6H_{15/2}$ transition. Factors that influence the yellow-to-blue intensity ratio (Y/B) were investigated.[5] The intensity of the hypersensitive transition varies with the environment more obviously. Furthermore, the line linking the yellow and blue wavelengths in the CIE (Commission Internationale de l'Eclairage, International Commission on Illumination) 1931 chromaticity diagram usually passes through the white light region. Therefore, by adjusting Y/B to a suitable ratio, the chromaticity coordinates of the phosphors containing Dy^{3+} can be adjusted to the white light zone and can be used for lighting. Based on this principle, we prepared a white light emitting high-pressure mercury lamp excited by mercury plasma and using Dy^{3+} as an activator.[6,7] In order to avoid the use of harmful mercury, mercury-free luminescence lamps are explored. For this purpose, we studied the VUV excitation spectra and visible emission spectra of some Dy^{3+} activated phosphors. We found that by mixing the yellow and blue light of some phosphors containing Dy^{3+} ion such as $M_5(PO_4)_3F{:}Dy$ excited with 147 nm or 172 nm wavelength, the chromaticity coordinates of the emitted light are located in the white light region as described later. Therefore, Dy^{3+} ions have potential application for mercury-free fluorescence lamp.

MATERIALS AND METHODS

Powder samples $M_{5\text{-}2x}Dy_xNa_x(PO_4)_3F$ (for M = Ca, Sr, Ba) were prepared by a high-temperature solid-state reaction technique. For M = Ca and Sr in $M_{5\text{-}2x}Dy_xNa_x(PO_4)_3F$, the alkaline earth ions are provided by MCO_3 and $MHPO_4 \cdot 2H_2O$, and PO_4^{3-} ions are also provided from $MHPO_4 \cdot 2H_2O$. For preparation of $Ba_{5\text{-}2x}Dy_xNa_x(PO_4)_3F$, Ba^{2+} and PO_4^{3-} are provided by $Ba(NO_3)_2$ and $(NH_4)_2HPO_4$, respectively. The stoichiometric mixtures of analytical-grade purity MCO_3 and $MHPO_4 \cdot 2H_2O$ (for M = Ca, Sr) [or $Ba(NO_3)_2$ and $(NH_4)_2HPO_4$], Na_2CO_3, NH_4F, (excess 10 mol%) and 99.9% purity Dy_2O_3 were heated at 1100°C for 2 hr under air atmosphere. The final products were obtained by washing the samples with distilled water and then drying. Beacuse trivalent Dy^{3+} ions are located on divalent M^{2+} sites, some sort of charge compensating defect will be built in the lattices, therefore Na^+ ions provided by Na_2CO_3 were added as a charge-compensating defect. Namely, $M_{5\text{-}2x}Dy_xNa_x(PO_4)_3F$ are prepared by the following reactions:

$$4(1-x)MCO_3 + 6MHPO_4 \cdot 2H_2O + 2NH_4F + xDy_2O_3 + xNa_2CO_3 \xrightarrow{1373K,\,2\mathrm{hr}}$$
$$2M_{5-2x}Dy_xNa_x(PO_4)_3F + 2NH_3 + 16H_2O + (4-3x)CO_2,\ \text{for}\ M = Ca, Sr$$

$$2(5-2x)Ba(NO_3)_2 + 6(NH_4)_2HPO_4 + 2NH_4F + xDy_2O_3 + xNa_2CO_3 \xrightarrow{1373K,\,2\mathrm{hr}}$$
$$2Ba_{5-2x}Dy_xNa_x(PO4)_3F + 14NH_3 + 10H_2O + xCO_2 + 4(5-2x)NO_2$$
$$+ (5-2x)O_2$$

The structure of the final products was examined by X-ray powder diffraction using CuK_α radiation on a Rigaku D/max 2200 vpc X-ray diffractometer (Tokyo, Japan). The results indicated that all samples $M_{5\text{-}2x}Dy_xNa_x(PO_4)_3F$ are of single phase and consistent with JCPDS standard card numbered 71-0881 [$Ca_5(PO_4)_3F$], 50-1744 [$Sr_5(PO_4)_3F$], and 71-1316 [$Ba_5(PO_4)_3F$], respectively. The dopant Dy^{3+} and Na^+ ions did not show obvious influence on the XRD patterns. As examples, the XRD (X-ray diffraction) patterns of samples $M_5(PO_4)_3F$ are shown in Figure 1.

The UV excitation and UV-excited emission spectra were recorded on a JOBIN YVON FL3-21 spectrofluorometer at room temperature, and a 450 W xenon lamp was used as the excitation source.

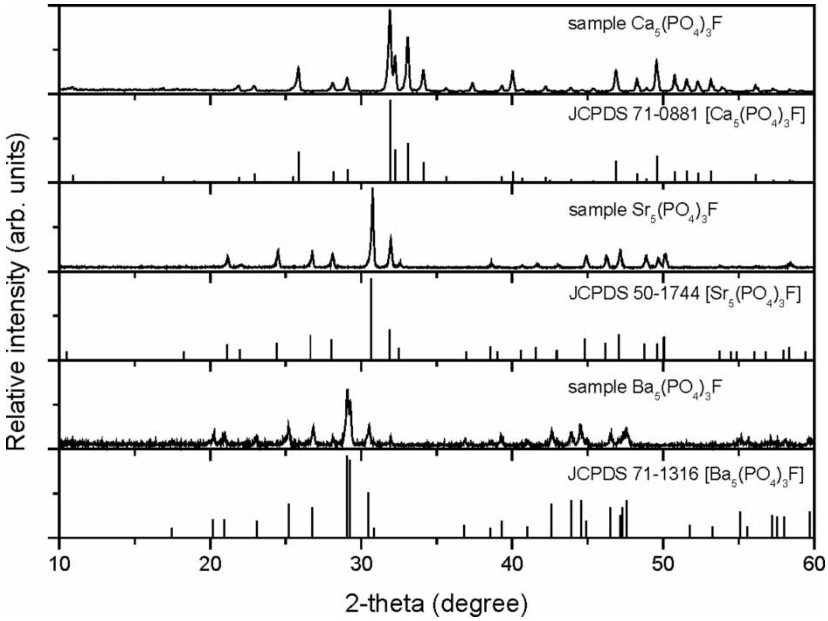

Figure 1. XRD patterns of samples $M_5(PO_4)_3F$ for M = Ca, Sr, Ba.

The VUV excitation and the VUV-excited luminescent spectra were measured at the time-resolved spectroscopy experimental station on beam line U24 of the National Synchrotron Radiation Laboratory (NSRL, Hefei, China) under normal operating conditions (the electron energy of the storage ring 800 MeV, the beam current about 100–200 mA, and the temperature 293 K). A Seya-Namioka monochromator (1200 g/mm, 100–400 nm) was used for the synchrotron radiation excitation photon, an ARC-257 monochromator (1200 g/mm, 330–700 nm) for the emission photon, and the signal was detected by a Hamamatsu H5920-01 photomultiplier. The resolution of the instruments is about 0.2 nm. The pressure in the sample chamber is about 1×10^{-3} Pa. The relative VUV excitation intensities of the samples are corrected by dividing the measured excitation intensities of the samples with the excitation intensities of sodium salicylate (o-$C_6H_4OHCOONa$) in the same excitation conditions.

RESULTS AND DISCUSSION

$Ca_{5-2x}Dy_xNa_x(PO_4)_3F$

The VUV-UV excitation spectra and the emission spectra under 172/352 nm VUV/UV excitation for the phosphor $Ca_{4.30}Dy_{0.35}Na_{0.35}(PO_4)_3F$ are shown in

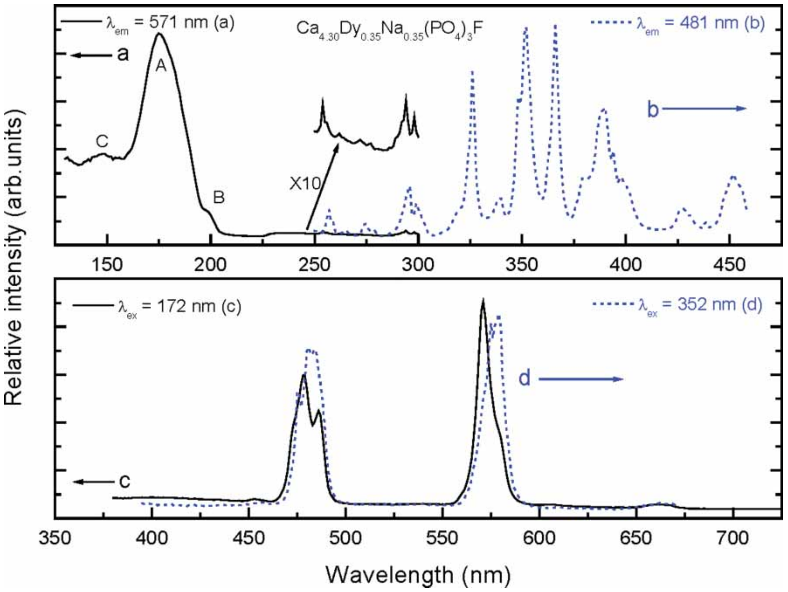

Figure 2. The VUV-UV excitation spectra and the emission spectra under 172/352 nm VUV/UV excitation for the phosphor $Ca_{4.30}Dy_{0.35}Na_{0.35}(PO_4)_3F$.

Figure 2. Curve b displays the UV excitation spectrum by monitoring the emission of Dy^{3+} at 481 nm. A series of absorption lines can be observed in the curve, which correspond with the intraconfigurational $4f^9 \rightarrow 4f^9$ transitions of Dy^{3+} in $Ca_5(PO_4)_3F$. The ground state of Dy^{3+} is $^6H_{15/2}$, the transition from this state to different excitation levels are read to be 257 ($^4P_{3/2}$), 274 ($^4G_{9/2}$, $^4G_{7/2}$), 296 ($^4K_{13/2}$, $^4H_{13/2}$, $^4F_{3/2}$, $^4D_{7/2}$), 326 ($^6P_{3/2}$), 340 ($^4F_{5/2}$, $^4I_{9/2}$, $^4G_{9/2}$), 352 ($^4I_{11/2}$, $^4M_{15/2}$, $^6P_{7/2}$), 366 ($^4P_{3/2}$, $^6P_{3/2}$, $^6P_{5/2}$), 390 ($^4M_{21/2}$, $^4I_{13/2}$, $^4F_{7/2}$), 427 ($^4G_{11/2}$), and 452 ($^4I_{15/2}$, $^4M_{19/2}$, $^4K_{17/2}$) nm, respectively, in Figure 2.

In curve a, the VUV excitation spectrum is presented. The weak f-f absorption lines in 250–300 nm range can be observed by multiplying this range 10 times in the curve. The positions of these lines are in agreement with that in curve b.

Comparing the 250–300 nm absorption intensities in curve a with that in curve b, we can deduce that the broad absorption band A with a maximum at about 175 nm in curve a is evidently stronger than the f-f transitions in curve b. The maximum position of VUV absorption is near the wavelength 175 nm, and meanwhile the absorption intensity is stronger when monitoring emission of Dy^{3+} at $\lambda_{em} = 571$ nm; these features suggested that the phosphor could efficiently absorb and transfer VUV activation energy to Dy^{3+} ions, which is advantageous to obtaining a higher efficiency VUV phosphor.

The band A is considered to include the host-related absorption, the f-d and the charge transfer (CT) transitions of Dy^{3+} in the host lattice from the following standpoints.

1. In our previous work,[8–10] the host-related absorption bands of some phosphates and fluorophosphates are investigated. Though the compositions and the structure of these phosphates and fluorophosphates are different, they all show absorption band around wavelength 150–170 nm. We consider that the intrinsic absorption of PO_4^{3-} is located around this range. Theoretical calculation[11] also confirmed that the lowest intramolecular $2t_2 \rightarrow 2a$, $3t_2$ transition energy of the tetrahedral PO_4^{3-} molecule was around 7–10 eV, [i.e. $\sim(56.4-80.6) \times 10^3\ cm^{-1}$ or $\sim$177–124 nm].
2. The f-d transitions of Dy^{3+} ions are complicated. First, the crystal field effect results in the splitting of 5d orbital into at most five states in terms of the lattice site symmetry. Second, when one electron is promoted from ground states $4f^9$ to $4f^85d^1$ of Dy^{3+}, it can give rise to two groups of f-d transitions: spin-allowed (SA) transitions are stronger and with higher energies, while spin-forbidden (SF) are weaker and with lower energies. So it is hard to unambiguously assign the f-d transitions. However, the energies of the lowest SA and the lowest SF f-d transitions can be evaluated according to the method proposed by Dorenbos and the spectroscopic data of Ce^{3+} ions in the host lattice.[12] The lowest 5d state energy is reported to be $49.34 \times 10^3\ cm^{-1}$ for free gaseous Ce^{3+}, while this energy is found around $32.26 \times 10^3\ cm^{-1}$ for Ce^{3+} in $Ca_5(PO_4)_3F$ in our work. Then, we can calculate that the decreasing of the lowest 5d state for Ce^{3+} in the host lattice (D value) is about $17.08 \times 10^3\ cm^{-1}$. Because the influence of the crystal field and covalency of the host lattice on the red shift of 4f5d levels are approximately equal for all rare-earth ions, we consider this D value is adopted by Dy^{3+} in $Ca_5(PO_4)_3F$. The energies of the lowest SA and the lowest SF f-d transitions for free Dy^{3+} ions are reported to be $74.44 \times 10^3\ cm^{-1}$ and $68.74 \times 10^3\ cm^{-1}$, respectively.[12] Then we predicate that the lowest SA and the lowest SF f-d transitions for Dy^{3+} ions in $Ca_5(PO_4)_3F$ are $57.36 \times 10^3\ cm^{-1}$ (174 nm, strong) and $51.66 \times 10^3\ cm^{-1}$ (193 nm, weak), respectively. The positions are near peak A (175 nm, strong) and band B (199 nm, weak), respectively.
3. The energy of charge transfer band (CTB) can be roughly estimated by the Jørgensen empirical formula:[13]

$$E_{CT} = [\chi_{opt}(X) - \chi_{opt}(M)] \times 30 \times 10^3\ cm^{-1}. \quad (1)$$

Here, E_{CT} gives the energy of CTB in units cm^{-1}, and $\chi_{opt}(X)$ and $\chi_{opt}(M)$ are the optical electronegativities of the anion X and central metal cation M, respectively. When M is lanthanide ion Ln^{3+}, suppose the change of $\chi_{opt}(X)$

for the anion X with the environment in different compounds A is greater than $\chi_{opt}(Ln^{3+})$ for the lanthanide cation because the p electrons in the anion X such as O are located at the outmost orbit and the f electrons in the lanthanide cation are shielded by the outer $5s^2$ and $5p^6$ shells. If we assume the value of $\chi_{opt}(Ln^{3+})$ keeps constant, the $\chi_{opt}(X, A)$ in compound A can be calculated from the measured CTB of Eu^{3+} in A and the value of $\chi_{opt}(Eu^{3+})$ as follows:

$$\chi_{opt}(X, A) = [E_{CT}(Eu^{3+}, A)/30 \times 10^3] + \chi_{opt}(Eu^{3+}).$$

In general, $E_{CT}(Eu^{3+}, A)$ can be measured easily by excitation spectrum; it can be used as reference to estimate the CTB of other lanthanide ions. Substituting these values of $\chi_{opt}(X, A)$ for compound A in the Jørgensen formula, the CTB of other lanthanide ions $E_{CT}(Ln^{3+})$ in compound A can be estimated by the formula:

$$\begin{aligned} E_{CT}(Ln^{3+}, A) &= E_{CT}(Eu^{3+}, A) + [\chi_{opt}(Eu^{3+}) - \chi_{opt}(Ln^{3+})] \times 30 \times 10^3 \\ &= E_{CT}(Eu^{3+}, A) + \Delta\chi_{Eu-Ln} \times 30 \times 10^3, \end{aligned} \tag{2}$$

where $\Delta\chi_{Eu\text{-}Ln} = \chi_{opt}(Eu^{3+}) - \chi_{opt}(Ln^{3+})$; that is, the difference between the electronegativities of Eu^{3+} and other lanthanide ions Ln^{3+}, which can be obtained from Refs. 14 and 15. For Dy^{3+} ion, $\Delta\chi_{Eu\text{-}Dy} = 1.74 - 1.21 = 0.53$, and $\Delta\chi_{Eu\text{-}Dy} \times 30 \times 10^3 = 15{,}900\ cm^{-1}$ (1.97 eV).

Furthermore, the CT energy of Ln^{3+} ions in the hosts A can be evaluated by two formulas as reported by Dorenbos.

$$\text{Formula 1:}^{[16]}\ E_{CT}(Ln^{3+}, A) = E_{CT}(Eu^{3+}, A) + \Delta E_{CT}(Ln^{3+}), \tag{3}$$

where $\Delta E_{CT}(Ln^{3+}) = E_{CT}(Ln^{3+},A) - E_{CT}(Eu^{3+},A)$. For Dy^{3+} ion, $\Delta E_{CT}(Dy^{3+}) = 2.04$ eV (16,452 cm^{-1}), which is the difference between the energy of the CTB to the Dy^{3+} with that to Eu^{3+} averaged over only four compounds.

$$\text{Formula 2:}^{[17]}\ E_{CT}(Ln^{3+}, A) = E_{CT}(Eu^{3+}, A) + \Delta E_{vf}(Ln^{2+}), \tag{4}$$

where $\Delta E_{vf}(Ln^{2+})$ denote the average energy difference between the ground state energy of $E_{vf}(Eu^{2+})$ and the ground state energy of other divalent lanthanide Ln^{2+} $E_{vf}(Ln^{2+})$, in which $E_{vf}(Eu^{2+})$ and $E_{vf}(Ln^{2+})$ represent the energy difference between the top of valence band and the 4f ground state of Eu^{2+} and Ln^{2+}, respectively. The values of $\Delta E_{vf}(Ln^{2+})$ can be obtained from Ref. 17 For Dy^{3+} ion, $\Delta E_{vf}(Ln^{2+}) = 2.28$ eV.

All Equations (2), (3), and (4) mentioned above have similar form as follows:

$$E_{CT}(Ln^{3+}, A) = E_{CT}(Eu^{3+}, A) + C(Ln^{3+}).$$

It means that the CTB of other Ln^{3+} appears always higher in a definite energy $C(Ln^{3+})$ than that of Eu^{3+}, where C (Ln^{3+}) is a value that depends on the $\Delta\chi_{\text{Eu-Ln}}$, $\Delta E_{CT}(Ln^{3+})$ or $\Delta E_{vf}(Ln^{2+})$ of the lanthanide ion used. For Dy^{3+} ion, $C(Dy^{3+}) = \Delta\chi_{\text{Eu-Dy}} \times 30 \times 10^3 = 15{,}900\ \text{cm}^{-1}$ (1.97 eV) in Eq. (2); $C(Dy^{3+}) = \Delta E_{CT}(Dy^{3+}) = 2.04$ eV (16,452 cm^{-1}) in Eq. (3): and C $(Dy^{3+}) = \Delta E_{vf}(Ln^{2+}) = 2.28$ eV (18,388 cm^{-1}) in Eq. (4).

The CTB of Eu^{3+} in $Ca_5(PO_4)_3F{:}Eu^{3+}$ has been measured by Sahoo et al.[18] The fluorapatites $M_5(PO_4)_3F$ (M = Ca, Sr, Ba) belong to the apatite structure which crystallizes in the hexagonal system with the space group corresponding with $P6_3/m$. Two types of M^{2+} ions occur in $M_5(PO_4)_3F$. M(I) ions are with ninefold oxygen coordination in high-symmetry C_3. M(II) ions are with sixfold oxygen and onefold fluorine coordination in low-symmetry C_s. Ln^{3+} can substitute for Ca^{2+} in position Ca(I) or Ca(II). For Eu^{3+} in Ca(I) of $Ca_5(PO_4)_3F$, the $E_{CT}(Eu^{3+})$ is 39,841 cm^{-1} (251 nm or 4.94 eV). For Eu^{3+} in Ca(II), the $E_{CT}(Eu^{3+})$ are 30,769 cm^{-1} (325 nm or 3.81 eV) and 35,714 cm^{-1} (280 nm or 4.43 eV), Substituting all these values into equations (2), (3), or (4), the calculated CTB positions of Dy^{3+} ion in Ca(I) and Ca(II) sites for $Ca_5(PO_4)_3F$ are shown in Table 1.

The calculated positions are very close to the experimental wavelengths of the bands A and B in Figure 2. The $E_{CT}(Dy^{3+}, Ca_5(PO_4)_3F)$ values obtained are nearly the same even if they are calculated by different methods. We calculated also the $E_{CT}(Dy^{3+}, LnCa_4O(BO_3)_3)$ from the datum of $E_{CT}(Eu^{3+}, LnCa_4O(BO_3)_3)$ by equations (2) and (4). Similar results were obtained.[19]

In addition, a weak band C (peaking at about 148 nm) can be observed in the curve a, which is probably related to the f-d transition of Dy^{3+} or unknown impurity and defects in the host lattice.

In general, the transitions from the excited state $^4F_{9/2}$ to the lower states ^6H_J ($J = 11/2, 13/2, 15/2$) occurred in visible (380–730 nm) range for Dy^{3+}

Table 1. The CTB positions of Dy^{3+} ion in Ca(I) and Ca(II) sites for $Ca_5(PO_4)_3F$ calculated by equations (2), (3), or (4)

	$E_{CT}(Dy^{3+}, Ca_5(PO_4)_3F)$ (nm)		
Site	(2)	(3)	(4)
Ca(I)	179	180	172
Ca(II)	214, 194	212, 192	204, 185

activated phosphors.[5–7] Among these transitions, the $^4F_{9/2}$-$^6H_{13/2}$ yellow transition belongs to the hypersensitive transition ($\Delta L = 2$, $\Delta J = 2$), which is strongly influenced by the environment. The $^4F_{9/2}$-$^6H_{15/2}$ blue transition belongs to the non-hypersensitive transition. Hence by mixing the yellow and blue emission at a suitable matrix with suitable yellow-to-blue intensity ratio Y/B, white light emission will be obtained. By a single matrix, the luminescent materials activated with only one dopant Dy^{3+} may be used as a potential white light emitting phosphor. To obtain white-emitting lighting by this approach, the consumption of rare earth raw materials is decreased compared with the tricolor phosphors. It is expected to obtain white light emitting phosphors more economically.

The emission spectra upon 352/172 nm UV/VUV excitation are exhibited in Fig. 2 curves c and d. All three $^4F_{9/2}$-^6H_J ($J = 11/2, 13/2, 15/2$) lines are observed in the curves, in which the blue $^4F_{9/2} \rightarrow {}^6H_{15/2}$ emission at about 480 nm and the yellow $^4F_{9/2} \rightarrow {}^6H_{13/2}$ emission at about 570 nm are strong, whereas the red $^4F_{9/2} \rightarrow {}^6H_{11/2}$ transition at about 660 nm is very weak. The positions of these lines under UV excitation are in agreement with that under VUV excitation, but the relative intensities show some differences as the different instrumental response of PMT. The chromaticity coordinates (x, y) and correlated color temperature (K) are calculated in terms of these curves, and the results are listed in Table 2 and are displayed in Figure 3, indicating the phosphor shows white light emission under UV/VUV excitation. The phosphor is probably a potential candidate for Hg-free lamp.

$Sr_{5-2x}Dy_xNa_x(PO_4)_3F$

The VUV-UV excitation spectra and the emission spectra under 172/351 nm VUV/UV excitation for the phosphor $Sr_{4.60}Dy_{0.20}Na_{0.20}(PO_4)_3F$ are displayed in Figure 4.

Table 2. The chromaticity coordinates (x, y) of phosphors $M_{5-2x}Dy_xNa_x(PO_4)_3F$ (M = Ca, $x = 0.35$; M = Sr, $x = 0.20$; M = Ba, $x = 0.25$) under VUV/UV excitation

Sample	Excitation wavelength (nm)	Chromaticity coordinates		Color temperature (K)
		x	y	
$Ca_{4.30}Dy_{0.35}Na_{0.35}(PO_4)_3F$	172	0.323	0.356	5882
	352	0.336	0.367	5384
$Sr_{4.60}Dy_{0.20}Na_{0.20}(PO_4)_3F$	172	0.305	0.343	6811
	351	0.348	0.374	4965
$Ba_{4.50}Dy_{0.25}Na_{0.25}(PO_4)_3F$	172	0.321	0.361	5979
	350	0.355	0.394	4808

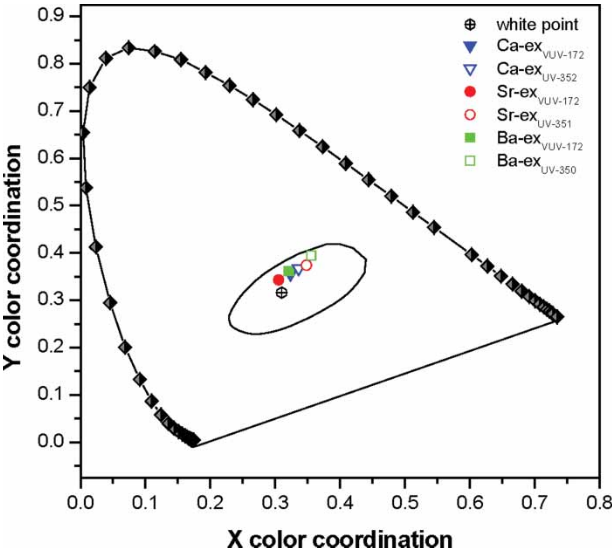

Figure 3. The chromaticity coordinates (x, y) of phosphors $M_{5\text{-}2x}Dy_xNa_x(PO_4)_3F$ (M = Ca, $x = 0.35$; M = Sr, $x = 0.20$; M = Ba, x = 0.25) in the CIE 1931 chromaticity diagram.

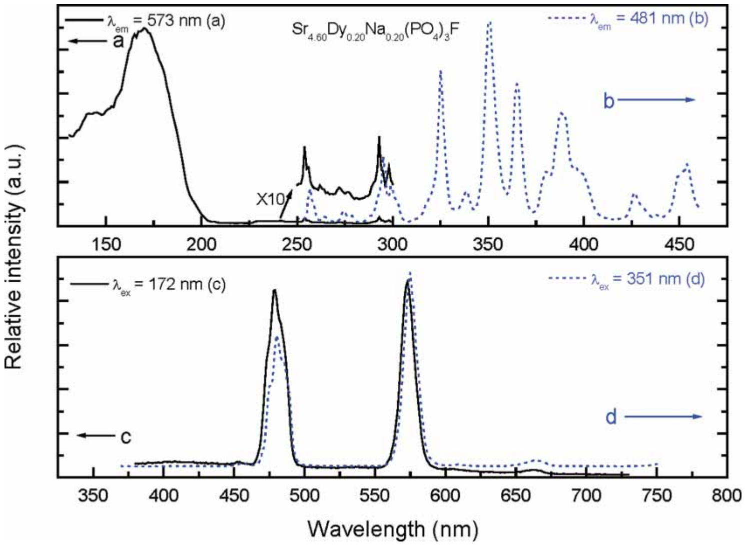

Figure 4. The VUV-UV excitation spectra and the emission spectra under 172/351 nm VUV/UV excitation for the phosphor $Sr_{4.60}Dy_{0.20}Na_{0.20}(PO_4)_3F$.

For curves a and b, the absorption lines in the wavelength range 250–460 nm are f-f transitions of Dy^{3+}, as mentioned in the above section. The broad bands below 200 nm are probably related to the host absorption, charge transfer, and f-d transitions of Dy^{3+} in the host lattice, which are discussed in the above section also.

Two strong lines and a weak line were observed in the emission curves c and d in Figure 4, whose positions are nearly the same as that of $Ca_{4.30}Dy_{0.35}Na_{0.35}(PO_4)_3F$ shown in Figures 2c and 2d. The chromaticity coordinates and correlated color temperature (K) are calculated according to these curves and displayed in Figure 3, showing the white light emission of the phosphor under UV/VUV excitation. At present, the quantum efficiency of the phosphors under VUV excitation is unknown because of the limitation of experimental conditions, and work on this issue will be conducted in the future.

$Ba_{5-2x}Dy_xNa_x(PO_4)_3F$

Figure 5 displays the VUV-UV excitation spectra and the emission spectra under 172/350 nm VUV/UV excitation for the phosphor $Ba_{4.50}Dy_{0.25}Na_{0.25}(PO_4)_3F$.

As discussed in the above sections, the broad bands in VUV excitation spectrum (curve a) probably include the host-related absorption, the CT and f-d transitions of Dy^{3+} in the matrix. The absorption lines in the 250–500 nm range are f-f transitions of Dy^{3+}. The chromaticity coordinates and

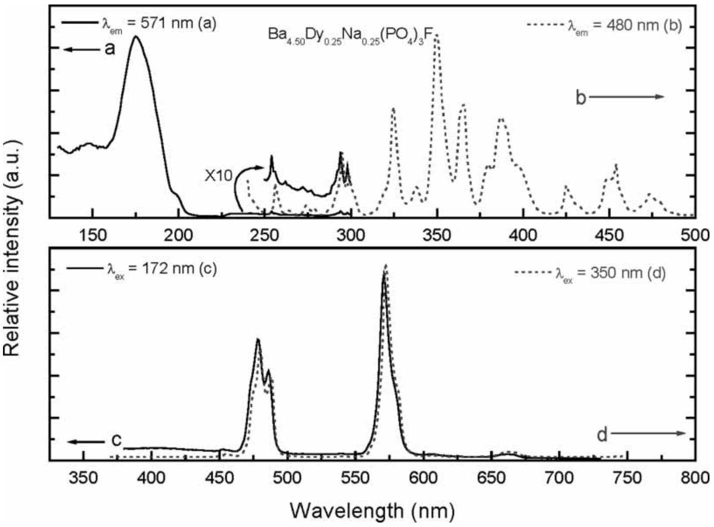

Figure 5. The VUV-UV excitation spectra and the emission spectrum under 172/350 nm VUV/UV excitation for the phosphor $Ba_{4.50}Dy_{0.25}Na_{0.25}(PO_4)_3F$.

correlated color temperature (K) are calculated by these curves and displayed in Figure 3.

Because the $^4F_{9/2} \rightarrow {}^6H_{11/2}$ transition at about 660 nm is very weak, here we just compare the influence of different M ions on the Y/B ratio of the relative intensity of yellow $^4F_{9/2} \rightarrow {}^6H_{13/2}$ transition (Y) to that of blue $^4F_{9/2} \rightarrow {}^6H_{15/2}$ transition (B) for Dy^{3+} in $M_5(PO_4)_3F$ (M = Ca, Sr, Ba). The results are listed in Table 3. First, it can be seen that the Y/B ratios show some difference for a specific phosphor under UV or VUV excitation, for example, the Y/B ratio is 1.048 under UV excitation, whereas it is 1.097 under VUV excitation for phosphor $Ca_{4.30}Dy_{0.35}Na_{0.35}(PO_4)_3F$, which is probably because of the different PMT response between the UV spectrofluorometer of our lab and the VUV instrument of NSRL. Second, upon UV excitation, the Y/B ratios are increased from Ca^{2+} to Sr^{2+} and Ba^{2+}. The similar tendency is observed under VUV excitation, though $Sr_{4.60}Dy_{0.20}Na_{0.20}(PO_4)_3F$ under VUV excitation is somewhat abnormal. From Ca^{2+} to Sr^{2+} and Ba^{2+} (electric charge $z = 2$), the ionic radii (r) increase as relative order $Ca^{2+} < Sr^{2+} < Ba^{2+}$, and the z/r and covalency degree of M-O bond decrease from Ca^{2+} to Sr^{2+} and Ba^{2+}. As $M_5(PO_4)_3F$ hosts share iso-structure, the result seems to suggest that the Y/B ratio increases with the increasing of M^{2+} ionic radii or the increasing of Dy-O bond covalency in the current case as indicated in Ref. 5.

The $^4F_{9/2}$-^6H_J (J = 11/2, 13/2, 15/2) emission intensities under 350-nm excitation of $Ba_{5-2x}Dy_xNa_x(PO_4)_3F$ samples as functions of Dy^{3+} concentration (x values) are shown in Figure 6. Owing to the cross-relaxation $^4F_{9/2} + {}^6H_{15/2} \rightarrow {}^6F_{3/2} + {}^6F_{11/2}$ that occurred, concentration quenching was observed in the samples. The emission is first increased and then decreased with the increasing of x value. The relative intensities of three transitions $^4F_{9/2}$-^6H_J (J = 11/2, 13/2, 15/2) show similar tendency with maximum intensity at $x = 0.25$. The emission intensity ratios Y/B are nearly independent on x as indicated previously in Ref. 5.

Table 3. Comparison of the yellow-to-blue relative intensity ratio ($^4F_{9/2} \rightarrow {}^6H_{13/2}/{}^4F_{9/2} \rightarrow {}^6H_{15/2}$) of phosphors $M_{5-2x}Dy_xNa_x(PO_4)_3F$ (M = Ca, $x = 0.35$; M = Sr, $x = 0.20$; M = Ba, $x = 0.25$) under VUV/UV excitation

Sample	Excitation wavelength (nm)	$^4F_{9/2} \rightarrow {}^6H_{13/2}$ (Y)	$^4F_{9/2} \rightarrow {}^6H_{15/2}$ (B)
$Ca_{4.30}Dy_{0.35}Na_{0.35}(PO_4)_3F$	352	1.048	1
$Sr_{4.60}Dy_{0.20}Na_{0.20}(PO_4)_3F$	351	1.175	1
$Ba_{4.50}Dy_{0.25}Na_{0.25}(PO_4)_3F$	350	1.317	1
$Ca_{4.30}Dy_{0.35}Na_{0.35}(PO_4)_3F$	172	1.097	1
$Sr_{4.60}Dy_{0.20}Na_{0.20}(PO_4)_3F$	172	0.876	1
$Ba_{4.50}Dy_{0.25}Na_{0.25}(PO_4)_3$	172	1.111	1

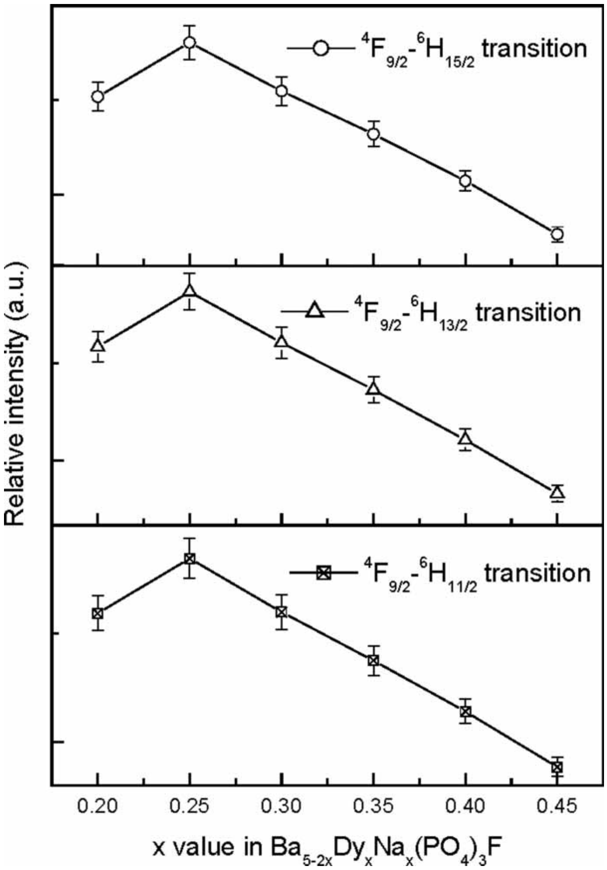

Figure 6. The $^4F_{9/2}$-^6H_J ($J = 11/2, 13/2, 15/2$) emission intensities as a function of Dy^{3+} concentration under 350 nm excitation.

CONCLUSIONS

A series of phosphors $M_{5\text{-}x}Dy_xNa_x(PO_4)_3F$ (M = Ca, Sr, Ba; x = 0, 0.02, 0.10, 0.15, 0.20, 0.25, 0.30, 0.35) were prepared by solid-state reaction technique at 1100°C. The VUV excitation spectra show that the phosphors exhibit a broad absorption band with a maximum near 172 nm, whose intensity is stronger than f-f transition intensities in the UV range. Upon VUV/UV excitation, the intense $^4F_{9/2} \rightarrow {}^6H_J$ ($J = 13/2, 15/2$) transitions and weak $^4F_{9/2} \rightarrow {}^6H_{11/2}$ transition were observed. The chromaticity coordinates of phosphors under VUV/UV excitation were calculated according to the emission spectra, showing that x, y values entered the white light region. Hence, the phosphors may be considered as candidates for Hg-free lamps, which are expected to be more economical than tricolor phosphor.

ACKNOWLEDGMENTS

This work was financially supported by the National Natural Science Foundation of China (grant no. 20571088), by the Science and Technology Project of Guangdong province (grant no. 2005A10609001, 2005B10301016), and by the NSRL innovation foundation of the Ministry of Education of China (grant no. 20051251S).

REFERENCES

1. Blasse, G.; Grabmaier, B. C. *Luminescent Materials*; Springer-Verlag: Berlin, 1994; pp. 115–122.
2. Shionoga, S.; Yen, W. M. *Phosphor Handbook*; CRC Press: Boston, 1999; pp. 389–432.
3. Jüstel, T.; Nikol, H.; Ronda, C. New development in the field of luminescent materials for lighting and displays. *Angew. Chem. Int. Ed.* **1998**, *37* (22), 3084–3103.
4. Jüstel, T.; Krupa, J.-C.; Wiechert, D. U. VUV spectroscopy of luminescent materials for plasma display panels and Xe discharge lamps. *J. Lumin.* **2001**, *93* (3), 179–189.
5. Su, Q.; Pei, Z.; Chi, L.; Zhang, H.; Zhang, Z.; Zou, F. The yellow-to-blue intensity ratio (Y/B) of Dy^{3+} emission. *J. Alloy. Compd.* **1993**, *192*, 25–27.
6. Su, Q.; Pei, Z.; Lin, J.; Xue, F. Luminescence of Dy^{3+} enhanced by sensitization. *J. Alloy. Compd.* **1995**, *225*, 103–106.
7. Su, Q.; Pei, Z.; Zeng, Q.; Chi, L.; Liu, S.; Lin, J.; Wang, S.; Lu, Y. Phosphors doped with Dy^{3+} and Gd^{3+} for lighting. *Mater. Sci. Forum.* **1999**, *315–317*, 228–235.
8. Liang, H. B.; Tao, Y.; Su, Q.; Wang, S. B. VUV-UV photoluminescence spectra of strontium orthophosphate doped with rare earth ions. *J. Solid State Chem.* **2002**, *167* (2), 435–440.
9. Liang, H. B.; Tao, Y.; Xu, J. H.; He, H.; Wu, H.; Chen, W. X.; Wang, S. B.; Su, Q. Photoluminescence of Ce^{3+}, Pr^{3+} and Tb^{3+} activated $Sr_3Ln(PO_4)_3$ under VUV-UV excitation. *J. Solid State Chem.* **2004**, *177* (3), 901–908.
10. Tian, Z. F.; Liang, H. B.; Lin, H. H.; Su, Q.; Guo, B.; Zhang, G. B.; Fu, Y. B. Luminescence of $NaGdFPO_4:Ln^{3+}$ after VUV excitation: a comparison with $GdPO_4:Ln^{3+}$ (Ln = Ce, Tb). *J. Solid State Chem.* **2006**, *179* (5), 1356–1362.
11. Saito, S.; Wada, K.; Onaka, R. Vacuum ultraviolet reflection spectra of KDP and ADP. *J. Phys. Soc. Jpn.* **1974**, *37* (3), 711–715.
12. Dorenbos, P. The 5d level positions of the trivalent lanthanides in inorganic compounds. *J. Lumin.* **2000**, *91* (3–4), 155–176.
13. Jørgensen, C. K. Electron transfer spectra of lanthanide complexes. *Mol. Phys.* **1962**, *5* (3), 271–277.
14. Su, Q.; Zhang, H. J.; Pei, Z. W.; Zou, F. Charge transfer bands of rare earth ions. In *Rare Earths Spectroscopy*; Su, Q., (ed.); Word Scientific: Singapore, 1990; pp. 214–223.
15. Su, Q. Optical electronegativity of lathanide ions. In *Proceedings of the 2nd International Conference on Rare Earth Development and Application*; Xu, G. X., Xiao, J. M., Yu, Z. S., and Chen, M. B., (eds.); International Academic Publishers: Beijing, P.R. China, 1991, Vol. 2; pp. 765–769.

16. Dorenbos, P. Systematic behavior in trivalent lanthanide charge transfer energies. *J. Phys. Condens. Matter* 2003 *15*, 8417–8434.
17. Dorenbos, P. The Eu^{3+} charge transfer energy and the relation with the band gap of compounds. *J. Lumin*; 2005; Vol. 111, pp. 89–104.
18. Sahoo, R.; Bhattacharya, S. K.; Debnath, R. A new type of charge compensating mechanism in $Ca_5(PO_4)_3F:Eu^{3+}$ phosphor. *J. Solid State Chem.* 2003 *175*, 218–225.
19. Yang, H. C.; Li, C. Y.; He, H.; Tao, Y.; Xu, J. H.; Su, Q. VUV-UV excited luminescent properties of $LnCa_4O(BO_3)_3:RE^{3+}$ (Ln = Y,La,Gd; RE = Eu,Tb,Dy,Ce). *J. Lumin.* 2006 *118*, 61–69.